JMBFS

Journal of Microbiology, Biotechnology and Food Sciences

International peer-reviewed scientific online journal

Published by Faculty of Biotechnology and Food Sciences

BIOCHEMICAL AND MECHANISTIC EVALUATION OF OLIVE LEAF EXTRACT-MEDIATED GREEN SYNTHESIZED ZNO NANOPARTICLES: ANTIDIABETIC POTENTIAL IN STZ-INDUCED RATS

Hadeer A. Omar[1,*], *Entsar A. Saad*[1], *Elshahat A. Toson*[1,†]

Address(es):
[1] Chemistry Department, Faculty of Science, Damietta University, Damietta, New-Damietta 34517, Egypt
[†] Deceased [12/1/2026]

*Corresponding author: hadeeromar23@du.edu.eg

https://doi.org/10.55251/jmbfs.14053

ARTICLE INFO

Received 4. 3. 2026
Revised 3. 5. 2026
Accepted 15. 5. 2026
Published 1. 6. 2026

Regular article

OPEN ACCESS

ABSTRACT

Olive leaves are a rich source of phytochemicals, particularly phenolic compounds and flavonoids with various biological activities. HPLC analysis confirmed that oleuropein was the predominant phenolic constituent in the extract. In this study, olive leaf extract (OLE) was utilized as a natural bio-reductant for the green synthesis of ZnO nanoparticles (OLE/ZnO-NPs). The antidiabetic potential of OLE and OLE/ZnO nanoparticles was evaluated using streptozotocin-induced diabetic rats, in addition to physicochemical characterization of the synthesized nanoparticles. UV–visible spectroscopy showed a new absorption peak at 350 nm, while FT-IR analysis indicated the involvement of the extract's functional groups in nanoparticle reduction and stabilization. TEM revealed spherical nanoparticles with an average size of 15–40 nm. Zeta potential analysis confirmed negatively charged particles (−15.58 ± 4.49 mV). *In vivo*, treatment with OLE/ZnO-NPs significantly reduced fasting blood glucose levels compared to diabetic controls. Improvements were also observed in HbA1c, insulin levels, adiponectin, leptin, and lipid profile, along with a reduction in the leptin/adiponectin ratio and insulin resistance index. *In vitro*, erythrocyte glucose uptake was significantly increased following treatment with the extract or its nano-formulation. These findings suggest that the antidiabetic effect of OLE and OLE/ZnO-NPs may be mediated through enhanced glucose uptake, improved antioxidant values, and modulation of adipokines.

Keywords: Olea europaea; Nanoparticles; Oleuropein; Antioxidants; Adipose cells

INTRODUCTION

Olea europaea leaves (olive leaves) are rich in bioactive molecules that may contribute to several biological properties. It demonstrates enormous economic and social significance and potential advantages of using any of its byproducts **(Gorzynik-Debicka *et al.* 2018)**. The therapeutic utilities of Olea europaea have been indicated in traditional medicine. It has been known to reduce blood sugar, cholesterol, and uric acid. It has also been used in ethnopharmacology to treat diabetes, hypertension, inflammation, diarrhea, respiratory and urinary tract infections, stomach and intestinal diseases, and as a vasodilator. According to **Al-Rejaboo *et al.* (2025)**, olive oil, fruit, and leaves have a long history of usage in medicine and provide a number of health benefits. People have used them as extracts, herbal teas, and powders in their diets **(Abugomaa and Elbadawy 2020)**. The bioactivity of extracts from olive tree byproducts appears to be caused by phenolic and antioxidant components, including oleuropein, hydroxytyrosol, oleuropein aglycone, and tyrosol **(Sánchez-Gutiérrez *et al.* 2021)**. It has anti-inflammatory, anti-cancer, antioxidant, and possible anti-diabetic effects **(Iantomasi *et al.* 2024)**. Better glucose metabolism has been linked to oleuropein. In diabetic rats, oleuropein has been shown to have an anti-hyperglycemic effect **(Basuny *et al.* 2023)**.

Medicinal plants have been used to cure a variety of human health issues, including diabetes. Several forms of diabetes exist and are caused by a complex mix of genetics, environmental factors, and lifestyle decisions **(Al-Saeed 2023)**. In diabetes mellitus (DM), high blood glucose levels are a hallmark of the disease. This illness affects the kidneys, eyes, blood vessels, and nervous system. Approximately 90% of people with diabetes are diagnosed with type 2 diabetes (T2D). This is linked to insulin dysfunction and fat buildup. The incapacity of insulin to carry out circulatory and metabolic functions in target tissues is known as insulin resistance **(Hassanien *et al.* 2020)**. A single, quick injection of streptozotocin (STZ) can experimentally cause DM by selectively killing the pancreatic β-cells which produce insulin **(Hassanien *et al.* 2020; Arivarasan *et al.* 2025).**

The growth and survival of life depend on the use of heavy metals, but in trace amounts. Heavy metals are known to be extremely poisonous to living things if taken in excess **(Al-Saeed 2023)**. Together with other heavy metals, including Cu, Pb, Ni, and Cd, zinc (Zn) is a component of the Earth's crust. Because zinc is a trace element that enhances the insulin signaling pathway and hepatic glycogenesis, it is a good choice for glucose metabolism **(Umrani and Paknikar 2014)**. Further, zinc oxide nanoparticles (ZnO-NPs) have a strong anti-diabetic impact by modifying glycemic parameters and lowering free radical production. Olive leaf extract, as one of the phytochemicals, was nano-formulated to increase its bioavailability, biodistribution, and anti-diabetic effects **(Basuny *et al.* 2023)**. Therefore, olive leaf methanolic extract (OLE) was used to greenly synthesize ZnO-NPs coated with OLE (OLE/ZnO-NPs).

White adipose cells (WAT) produce adiponectin (ADP) **(Khoramipour *et al.* 2021)**. It binds to its two main receptors, AdipoR1 and AdipoR2, to regulate insulin sensitivity, inflammation, whole-body energy, and fat-burning process **(Habib *et al.* 2015; Peng *et al.* 2018)**. The liver is the primary location for the expression of AdipoR2, which has the ability to deactivate PPAR-α (Peroxisome proliferator-activated receptors type alpha) receptors. This expression raises insulin sensitivity **(Saad *et al.* 2017)**. By decreasing gluconeogenesis as well as increasing glycolysis and lipid oxidation in the liver's cells, ADP helps regulate glucose absorption and lipid metabolism. AdipoR1 and hepatic AdipoR2 interact to produce these metabolic effects **(Yang *et al.* 2017)**.

The main function of leptin, as a hormone mostly produced by adipose tissue, is to regulate lipid reserves **(Picó *et al.* 2022)**. It was previously found that leptin expression in adipose tissue exhibits diurnal fluctuations and is controlled by numerous factors, including insulin, glucocorticoids, and catecholamines **(Nozhenko *et al.* 2015)**.

Oxidative stress is characterized by either a reduction in antioxidant defenses or an excess of free radicals, both of which contribute to elevated levels of radical species and therefore oxidative imbalance. The pathophysiology of diabetes mellitus is significantly influenced by oxidative stress in cells and tissues **(Habib *et al.* 2015; Elneely *et al.* 2025)**.

Despite growing interest in the antidiabetic potential of olive leaf extract and its bioactive constituents, the underlying mechanisms of action have not been fully elucidated. Therefore, the objective of our study was to provide a comprehensive evaluation integrating both *in vitro* and *in vivo* approaches to explore the metabolic, oxidative, biochemical, and histological mechanisms to elucidate how ZnO nanoparticles may potentiate the pharmacological activity of olive leaf constituents in diabetic rats. This integrative design aims to integrate cellular findings and whole-animal outcomes, offering a holistic understanding of its therapeutic potential in diabetes management through its abilities to improve erythrocyte uptake of glucose, hyperlipidemia, and insulin resistance.

MATERIAL AND METHODS

Materials

Sigma-Aldrich, a USA chemical manufacturer, supplied STZ and zinc acetate dihydrate. Novo Nordisk Egypt provided Act Rapid Insulin (1 ml, 100 IU human insulin). Commercial enzyme kits from the Bio Diagnostic Company in Cairo, Egypt were used to evaluate the alanine transaminase (ALT) and aspartate transaminase (AST) activities, albumin, total protein, creatinine, urea, uric acid, and lipid profile levels. As directed by the manufacturer, serum levels of insulin, ADP, and leptin were measured using ELISA kits for rat insulin, ADP, and leptin (ELK Biotechnology CO. Ltd.).

Extraction of olive leaves

Fresh leaves were taken from olive trees irrigated in the Faculty of Science, Damietta University, Egypt. They were cleaned by repeated washing under running water, and then using distilled water to get rid of any particles. For seven days, leaves were left to dry in the shade at ambient temperature. Using a hot plate stirrer, 10 g of leaves and 100 ml of 80% methanol were heated to 60 °C for two hours. After cooling, Whatman filter paper No. 1 was used to filter the mixture, which was then stored at 4°C for later use **(Kiritsakis *et al.* 2010).**

Determination of components of Olive Leaf Extracts using High-performance liquid chromatographic (HPLC)

The identification of the bioactive components of the methanolic extract of OLE was performed using a 20 µl sample (Agilent HPLC model No. 1100). The elution was carried out at room temperature at a flow rate of 1.00 ml/min.

Preparation of OLE/ZnO-NPs

According to **Gnanasangeetha and SaralaThambavani (2013),** zinc acetate dihydrate $Zn(CH_3COO)_2.2H_2O$ was used to create ZnO-NPs. To summarize, OLE was combined with a 0.01 M zinc acetate solution. Using 2 M NaOH, the mixture's pH was brought to 12. After that, the mixture was heated to 70°C and agitated for four hours. Following centrifugation for 15 minutes at 10,000 rpm, the resultant white precipitate was cleaned twice with sterile deionized water and dried overnight at 50 °C.

Characterization of OLE/ZnO-NPs

The generated nanoparticles' physical characteristics and chemical makeup, including size, nature of the surface, structure, and morphology, were determined using a UV-VIS (JASCO V-630) double-beam spectrophotometer. The absorption values were re-plotted using Origin Pro 8 software. FT-IR (Fourier Transform Infrared) spectrophotometer (JASCO FT/IR-4100, Japan). TEM (Transmission Electron Microscopy) at the Electron Microscope Unit, Damietta University, Egypt, using Malvern Instruments Ltd. The average hydrodynamic size, zeta potential, and the polydispersity index (PDI) were determined using Zetasizer Nano-ZS90 software (Version 2.3). The surface energy of the produced ZnO nanoparticles in solution was measured using the zetapotential method (Kassel, Germany).

Animals

This study followed the National Institute of Health's (NIH) guidelines. 30 Male albino rats Wistar strain (150–180 g) were acquired from the animal station in Abo Rawash, Egypt, and allowed to acclimate for 14 days at a temperature of 25 ± 3.2 °C with 12/12-hour cycles of light and dark. Every rat was housed in a hygienic polypropylene cage and given unlimited access to food and drink. All animal experiments are carried out according to the Guide for the Care and Use of Laboratory Animals, according to the IACUC, approved by the Institutional Review Board of the Faculty of Medicine (No. DFM-IRB 00012367-25-07-022, Issuing: 10 August 2025).

Design

The male rats received a single dose of STZ via intraperitoneal injection (i.p.) (Sigma, Chemical) at the conclusion of the acclimation period (14 days). STZ was freshly prepared immediately prior to administration, and the solutions were kept on ice and protected from light. STZ (50 mg/kg) was dissolved in sodium citrate buffer (0.1 mol/liter, pH 4.5). On the day of STZ administration, rats were provided with 5% glucose solution instead of regular drinking water to prevent severe hypoglycemia. **(Saad *et al.*, 2015)**. Within three to five days, STZ causes diabetes by killing the pancreatic beta cells. A blood glucose test meter (blood glucose meter, auto code series precichek AC-302, Germany) was used to monitor blood glucose. For the subsequent study, animals with glucose levels more than 300 mg/dL were chosen then received treatments daily for 4 weeks. Five groups of six rats each were randomly selected from the animals. G1: The healthy control group was fed only regular food. G2: Diabetic control (50 mg STZ/kg; i.p single injection), G3: Insulin-treated group (50 mg STZ/kg; i.p single injection), and subcutaneously treated with 4 IU/kg insulin **(Al-Saaidi *et al.*, 2014)**. G4: Oral extract group (50 mg STZ/kg; i.p single injection), and orally treated, by intragastric gavage, with 400 mg/kg extract **(Al-Attar & Alsalmi, 2019)**. G5: OLE/ZnO-NPs-treated group (50 mg STZ/kg; i.p single injection), and treated with 40 mg/kg OLE/ZnO NPs **(Virgen-Ortiz *et al.*, 2020)**.

Samples

After fasting for 6-8 h, tail vein blood was used to estimate FBG. Further, after 1 and 2 h of meal intake, other blood samples were obtained to estimate random and postprandial blood sugar, respectively. Following an 8-hour fast, all animals were sacrificed in accordance with the IACUC on the 30th day of the experiment. Clean, dry tubes containing or lacking EDTA were used to collect whole blood and serum, respectively, following a 15-minute centrifugation at 4000 rpm. For use in subsequent biochemical tests, the sera were separated and kept at -20°C.

Glucose tolerance test

All animals were fasted for 6-8 h, then received glucose (2 g/kg) orally by gavage. Blood samples were collected via the tail vein at 0, 60, and 120 min for glucose measurement after glucose loading **(Meighan *et al.* 2025)**. Glucose tolerance was assessed after i.p. administration of OLE/ZnO NPs or insulin to the diabetic rats. On the other hand, OLE was orally administered. 3 blood samples/rat (as mentioned before) were taken to construct this glucose tolerance curve using the method of **Trinder (1969).**

Determination of oxidative stress biomarkers in liver tissues

A known weight of the rat's liver tissues was washed 3 times with normal saline. Then, this tissue was weighed and homogenized in ice-cold phosphate buffer (50 mM, pH 7.5). The final homogenate (10%, w/v) was centrifuged in a cooling centrifuge at 12,000 rpm for 20 minutes at 4°C. After that, the upper layer was gathered and kept at -20°C for later use in estimations. Superoxide dismutase (SOD) and catalase (CAT) activities as well as reduced glutathione (GSH), malondialdehyde (MDA), total antioxidant capacity (TAC) and nitric oxide (NO) levels were determined according to the methods of **(Sinha 1972; Uchiyama and Mihara 1978; Paoletti *et al.* 1986; Koracevic 2001; Rahman *et al.* 2006; Menaka *et al.* 2009),** respectively.

Biochemical assessment of liver glycogen

With minor adjustments, the Carroll technique was used to calculate the hepatic glycogen concentration (**Carroll *et al.* 1956**). Briefly, glycogen was extracted from liver tissue by boiling with 30 % KOH and determined after alcohol precipitation. The precipitate was treated with phenol and sulfuric acid for quantification instead of the anthrone reagent. The calibration curve was constructed using glycogen (Sigma) as the standard. The amount of glycogen was measured in milligrams per gram of liver tissue.

Histological studies

Samples of liver, kidney, and pancreatic tissue preserved in 10% neutral formalin buffer were utilized. They gradually dried and cleaned in ethanol (70%) and xylene. After that, they were infiltrated with paraffin wax. Hematoxylin & eosin dyes were used to stain 5µm paraffin sections for microscopic inspection. Also, periodic acid–Schiff (PAS) staining was used to detect the amount of glycogen in the liver tissues of all animal groups using the method of **Hui *et al.* (2017**).

Estimation of erythrocytes-glucose uptake

Using the Jain technique, phosphate-buffered saline (PBS) was used three times to wash the erythrocytes of diabetic rats and controls. The washed cells were inoculated with 350 mg glucose/dL PBS for two hours at 37°C **(Jain 1989**). The ability of the cleaned erythrocytes to absorb glucose from a PBS solution with a specific glucose concentration was assessed. By subtracting glucose's optical density acquired after (final) incubation from that obtained before (initial) incubation, the amount of remaining (unconsumed) glucose can be calculated.

$$\text{\% of glucose uptake value} = \frac{\text{Initial glucose} - \text{final glucose}}{\text{Initial glucose}} \text{X } 100$$

Statistical analyses

Results are expressed as mean ± SD. One way ANOVA followed by Tukey's post hoc test was used for multiple comparisons. Statistical significance was set at $p \leq 0.05$. Analyses were conducted using SPSS (version 20). GraphPad Prism 6.0 software (La Jolla, CA, USA) was used to determine the area under the curve (AUC) for these two hours.

RESULTS

Analyzing olive leaf extract by HPLC

HPLC analysis showed the presence of several phenolic compounds including; oleuropein 35.41 µg/ml, pyrogallol 25.29 µg/ml, syringenic 15.74 µg/ml, benzoic acid 10.33 µg/ml, catechin 9.75µg/ml, cinnamic 5.76 µg/ml, chlorogenic 4.62 µg/ml, ferulic 4.07 µg/ml, salicylic acid 2.09 µg/ml, etc. In addition, flavonoidal compounds were also detected. These include: kampferol 13.91 µg/ml, naringin 8.09 µg/ml, myricetin 6.21 µg/ml, 7-OH luteolin 5.87 µg/ml, flavone 5.02 µg/ml, etc. (**fig. 1**).

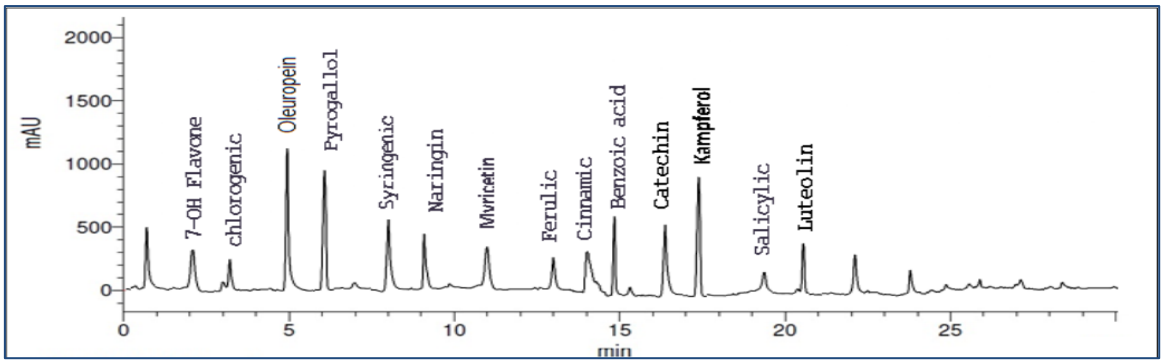

Figure 1 HPLC of phenolic and flavonoidal compounds of methanolic olive leaves extract.

ZnO-NPs characterization

The optical characteristics of OLE/ZnO-NPs were examined using a double-beam UV-Vis spectrophotometric technique. When these nanoparticles were being prepared, color changes were visually detected by forming a white precipitate. The OLE/ZnO NPs' new absorption peak was detected at 350 nm (**fig. 2A**).

FT-IR spectroscopy of OLE revealed bands at 3545.49 cm^{-1}, 2922.59 cm^{-1}, 1749.12 cm^{-1}, 1607.38 cm^{-1} and 1080.91cm^{-1}, corresponding to -OH, C-H, C=O, C=C, and C-O stretching, respectively; confirm structure of oleuropein (**fig. 2B**). The wave-number range of this functional group was 400 to 4000 cm $^{-1}$(one cm^{-1} resolution). Moreover, FT-IR spectroscopy of OLE-ZnONPs revealed bands at 3394.1 cm^{-1}, 1036.55 cm^{-1}, 1513.85 cm^{-1} and 2931.27 cm^{-1} confirm -OH stretch of polyphenols, C-O stretching, C=C and C-H alkaline vibrations, respectively. The absorption bands from 900-400 cm^{-1} (875.524 cm^{-1}, 555.398 cm^{-1} , and 417.513 cm^{-1}) confirm the formation of ZnO-NPs (**fig. 2C**).

TEM and zeta analyses were used to characterize OLE/ZnO-NPs shape, size, distribution, and potential. TEM micrograph of OLE/ZnO-NPs showed successful green synthesis of crystalline, cubic-shaped NPs with an average size ranging from 15 to 40 nm (**fig. 2D**). Zeta potential of the surface charge of the prepared materials was (≈ -15.58±4.49 mV) as shown in **fig. 2E**. The Zeta distribution average size reached to 473.2 nm for OLE/ZnO-NPs (**fig. 2F**). We employed TEM and zeta studies to look at the shape, size, distribution, and potential of OLE/ZnO-NPs. The result for the poly-dispersity index (PDI) is 0.0326.

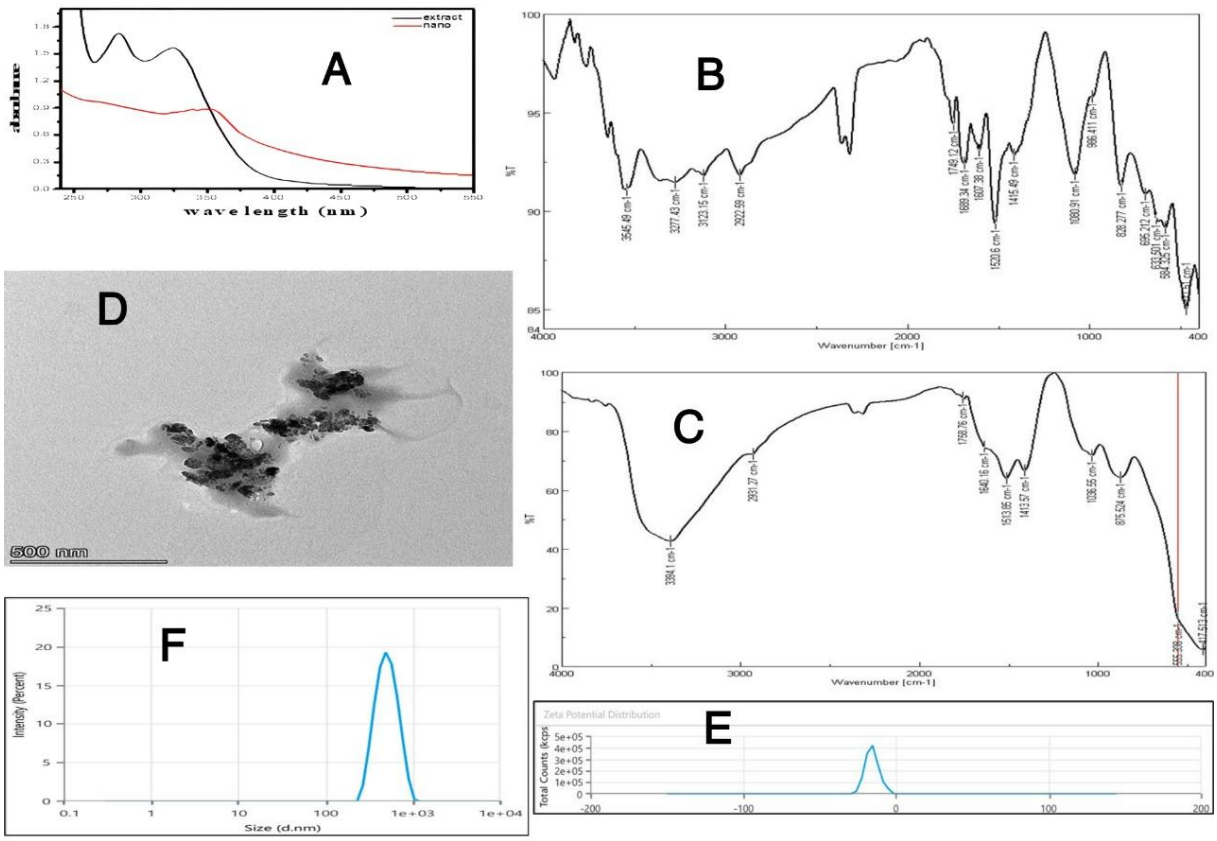

Figure 2 (A) The ultraviolet-visible absorption bands of OLE/ZnO-NPs solution, (B) FT-IR absorption spectrum for OLE, (C) FT-IR spectrum of olive leaf extract-mediated zinc oxide nanoparticles (OLE/ZnO NPs), (D) TEM picture of the greenly prepared OLE/ZnO-NPs, (E) Zeta potential of the prepared OLE/ZnO-NPs, (F) Zeta distribution of the prepared OLE/ZnO-NPs.

Effects of OLE, OLE/ZnO-NPs and insulin treatments on FBG, HbA1c, insulin levels and HOMA-IR

Intraperitoneal injection of STZ into rats was employed to cause diabetes. The mean FBG levels in the whole blood of diabetic rats was significantly higher than those of healthy rats, according to the data (M±SD= 81.33±9 mg/dL; p<0.001). When the mean FBG level in olive leaf extract or OLE/ZnO-NPs treated rats were compared with that of diabetic-untreated rats (477.67±30.4 mg/dL), the former groups showed statistically significant decreases, especially those which were treated with the OLE/ZnO-NPs (281.67±34.3 and 258.83±26.8 mg/dL,

respectively; p<0.001). The mean values of HbA1c, insulin, and HOMA-IR showed similar outcomes (**fig. 3)**.

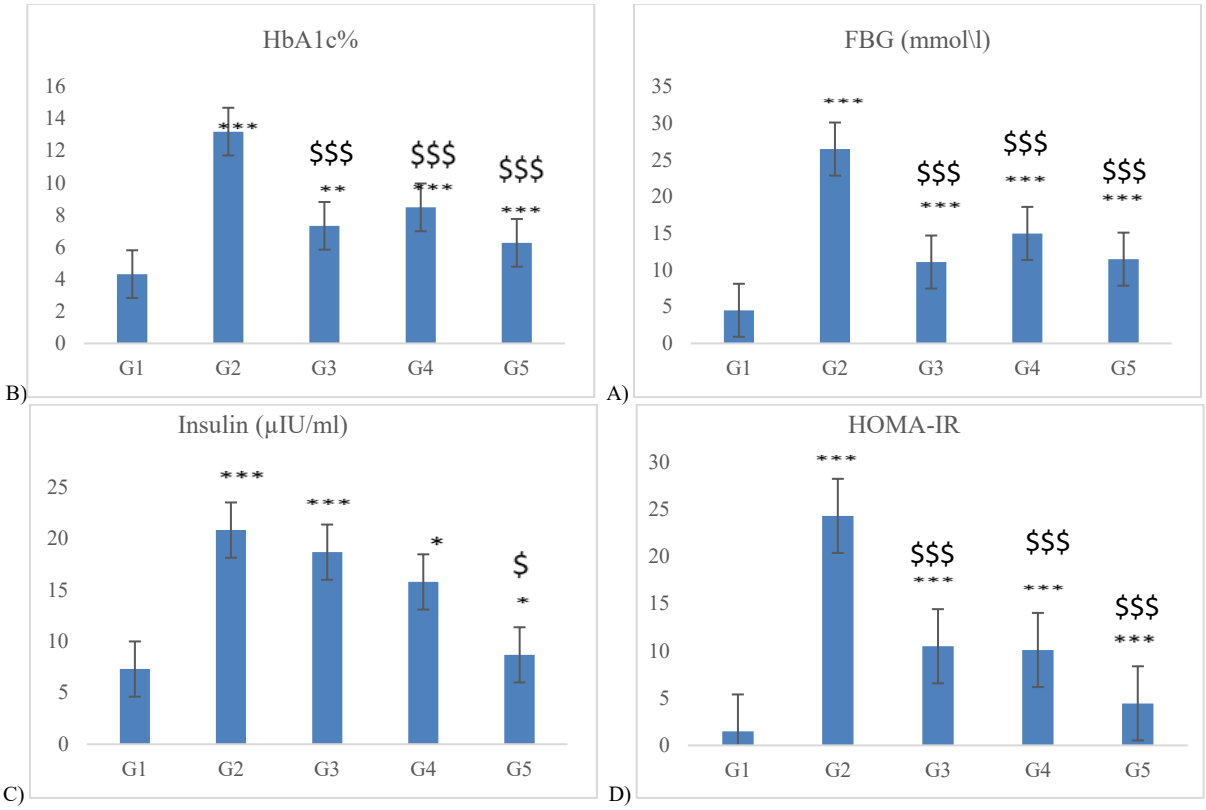

Figure 3 Effects of olive leaf extract (OLE), OLE/ZnO-NPs, and insulin on fasting blood glucose (FBG; A), glycated hemoglobin (HbA1c; B), insulin levels (C) and homeostatic model assessment for insulin resistance (HOMA-IR; D). *G1 (healthy control group), G2 (Diabetic control group), G3 (Sc-insulin-treated group), G4 (Oral OLE-treated group), G5 (i.p. OLE/ZnO-NPs-treated group).* Statistical significance vs. healthy control is indicated by * (p < 0.05), ** (p < 0.01), and *** (p < 0.001). Statistical significance vs. diabetic control is indicated by $ (p < 0.05), $$ (p < 0.01), and $$$ (p < 0.001). ns = p > 0.05.

With respect to glucose tolerance testing, blood glucose levels were measured at 0, 60, and 120 minutes for all experimental groups. As expected, the mean levels of glucose were the highest at 60 minutes post-glucose administration. After 120 minutes, the mean blood glucose levels in treated rats were nearly normalized compared to the diabetic group (**fig. 4 a**).
results of these AUCs were depicted in **fig. 4 b**.

From the results of **fig. 4 a**, the areas under each curve (AUC) were calculated. When compared to the normal control group, the AUC of diabetic rats was found to be considerably higher (p<0.001). In addition, the AUC of diabetic rats that were treated with insulin, OLE and OLE/ZnO-NPs were extremely significantly decreased (p<0.001) when compared to that of the untreated diabetes-induced rats. The

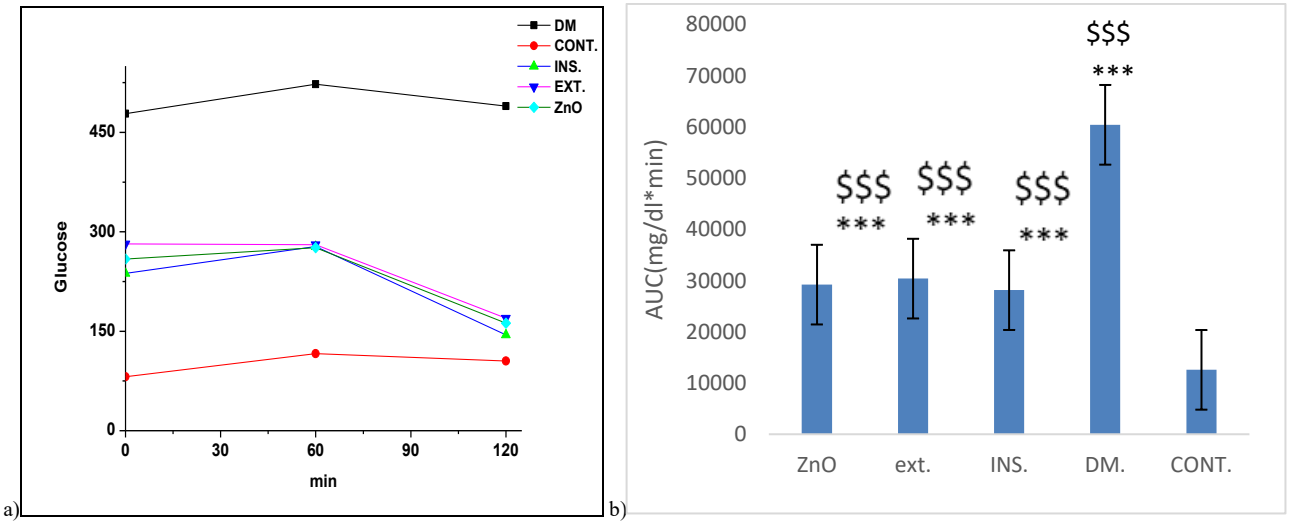

Figure 4 Glucose tolerance test. Effect of OLE, OLE/ZnO-NPs and insulin (INS) on blood glucose tolerance curve (a), calculated area under curves (AUCs) in control, diabetic and treated rats (b). *ZnO= Olive leaf extract-zinc oxide nanoparticles-treated group, ext= olive leaf extract-treated group, INS= Insulin-treated group, DM=diabetes mellites group, CONT=healthy control group.* Statistical significance vs. healthy control is indicated by * (p < 0.05), ** (p < 0.01), and *** (p < 0.001). Statistical significance vs. diabetic control is indicated by $ (p < 0.05), $$ (p < 0.01), and $$$ (p < 0.001). ns = p > 0.05.

The results of **table 1** showed an extremely significant decrease in leptin level in OLE and OLE/ZnO-NPs treated diabetic rats (16.3±8.6 and 12.27±6.18 ng/ml; p<0.001; p <0.05, respectively) when compared with that of diabetic-untreated rats (27.76±4.15 ng/ml). Similar results were noted for LAR. On the other hand, the results were noted for the mean ADP level in sera of OLE/ZnO-NPs treated diabetic rats were very significantly increased (32.54±6 ng/ml; p<0.05) when compared to the untreated diabetic rat (table 1).

The mean total cholesterol (T.C.), Triglycerides (T.G.), LDL, VLDL, and total lipid levels in sera of diabetic rats treated with OLE were 225.66±8.98, 175±63.7, 156.6±14, 35±12.7, and 763.88±145 mg/dL, respectively. Notably, in OLE/ZnO-NPs treated diabetic rats, these levels were 193.6±10.99, 138.1±45, 130.5±17.7, 27.6±9, and 523.7±152.3 mg/dL, respectively. When these results were compared to those of the untreated diabetic rat (343.6±104.2, 376.4±29.4, 249.5±109.7,

71.9±8.16, and 1229.39±392.6 mg/dL, respectively), the results were significantly decreased (table 2).

Table 1 Effect of olive leaf extract (OLE), OLE/ZnO-NPs and insulin on levels of adiponectin (ADP), leptin and leptin/adiponectin ratio (LAR).

variables	ADP *(ng/ml)*	Leptin (*ng/ml)*	LAR
G1	66.84±15.3	2.69±0.5	0.043±0.02
G2	23.4±7.06***	27.76±4.15***	1.33±0.6***
G3	35.8±5.9$^{***, ns}$	18.4±5.3$^{***, \$}$	0.54±0.2$^{ns, \$\$}$
G4	29.91±3.16$^{***, ns}$	16.3±8.6$^{***, \$\$}$	0.58±0.4$^{*, \$\$}$
G5	32.54±6$^{***, \$}$	12.27±6.18$^{*, \$\$\$}$	0.41±0.3$^{*, \$\$\$}$

G1 (healthy control group), G2 (Diabetic control group), G3 (Sc-insulin-treated group), G4 (Oral OLE-treated group), G5 (i.p. OLE/ZnO-NPs-treated group*). Statistical significance vs. healthy control is indicated by * (p < 0.05), ** (p < 0.01), and *** (p < 0.001). Statistical significance vs. diabetic control is indicated by $ (p < 0.05), $$ (p < 0.01), and $$$ (p < 0.001). ns = p > 0.05.*

The mean activities of ALT and AST in diabetic rats treated by OLE and OLE/ZnO NPs were extremely significantly decreased (p<0.001), but the mean levels of albumin and total proteins were very significantly increased when compared to those of the diabetic untreated rats. In addition, the mean levels of urea, uric acid, and creatinine in sera of diabetic rats, which were treated by OLE and OLE/ZnO-NPs were extremely significantly decreased (p<0.001) when compared to those of the diabetic untreated rats (table 3).

Table 2 Effect of OLE, OLE/ZnO NPs and insulin treatments on lipid profile.

variables	G1	G2	G3	G4	G5
Total cholesterol *(mg/dL)*	82.11±29.3	343.6±104.2***	253.8±33.7$^{***, \$\$}$	225.66±8.98$^{***, \$\$}$	193.62±10.99$^{***, \$\$\$}$
Triglycerides *(mg/dL)*	74±15.7	376.4±29.4***	203.67±41.3$^{***, \$\$\$}$	175±63.7$^{***, \$\$\$}$	138.06±45.05$^{ns.,\$\$\$}$
HDL*(mg/dL)*	41.63±8.49	22.15±1.75***	29.57±6.87$^{***, \$}$	34.01±6.9$^{ns., \$}$	35.53±4.8$^{ns., \$}$
LDL*(mg/dL)*	25.68±18.7	249.5±109.7***	183.5±29.4$^{***, \$}$	156.6±14.1$^{***, \$}$	130.49±17.7$^{**, \$\$\$}$
VLDL*(mg/dL)*	14.8±3.15	71.9±8.16***	40.73±8.26$^{***, \$\$\$}$	35±12.7$^{**, \$\$\$}$	27.6±9$^{ns.,\$\$\$}$
Total lipid *(mg/dL)*	382.69±66.6	1229.39±392.6***	829.95±87.7$^{***, \$\$\$}$	763.88±145$^{*, \$\$}$	523.7±152.3$^{ns.,\$\$\$}$

*G1 (healthy control group), G2 (Diabetic control group), G3 (Sc-insulin-treated group), G4 (Oral OLE-treated group), G5 (i.p. OLE/ZnO-NPs-treated group). HDL (high density lipoprotein), LDL (low density lipoprotein), VLDL (very low density lipoprotein). Statistical significance vs. healthy control is indicated by * (p < 0.05), ** (p < 0.01), and *** (p < 0.001). Statistical significance vs. diabetic control is indicated by $ (p < 0.05), $$ (p < 0.01), and $$$ (p < 0.001). ns = p > 0.05.*

Table 3 liver and kidney function tests in control, diabetic and treated groups.

Variables	G1 (n=6)	G2 (n=6)	G3 (n=6)	G4(n=6)	G5(n=6)
Liver function tests					
ALT *(U/ml)*	33.31±11.65	111.74±16.2***	38.85±17.9$^{ns, \$\$\$}$	55.32±22.5$^{ns, \$\$\$}$	43.73±8.69$^{ns, \$\$\$}$
AST (*U/ml*)	43.43±17.35	133.68±30.1***	52.6±10.38$^{ns, \$\$\$}$	61.35±23.8$^{ns, \$\$\$}$	51.18±7.4$^{ns, \$\$\$}$
Albumin *(g/dL)*	3.02±0.36	2.19±0.36***	2.82±0.15$^{ns, \$\$}$	2.29±0.36**	2.35±0.34$^{**, ns}$
Total Proteins *(g/dL)*	6.2±0.89	3.16±1.66**	5.98±1.04$^{ns, \$\$}$	4.93±1.97^{ns}	5.44±1.29$^{ns, \$}$
Kidney function tests					
Creatinine *(mg/dL)*	0.39±0.2	3.57±1.28***	0.51±0.24$^{ns, \$\$\$}$	0.99±0.35$^{ns, \$\$\$}$	2.16±0.73$^{***, \$\$}$
Uric acid *(mg/dL)*	2.99±0.32	9.88±1.5***	3.38±0.22$^{ns, \$\$\$}$	4.56±0.51$^{**, \$\$\$}$	5.69±0.72$^{***, \$\$\$}$
Urea *(mg/dL)*	31.78±5.8	189.6±39.7***	79,6±8.5$^{***, \$\$\$}$	95.33±8.4$^{***, \$\$\$}$	125.38±8.9$^{***, \$\$\$}$

*-n= number (6 rats each) -values were expressed as mean±standard deviations - G1: healthy control group, G2: Diabetic control group, G3: Sc-insulin treated group, G4: Oral OLE-treated group, G5: i.p. OLE/ZnO-NPs-treated group. ALT (Alanine aminotransferase), AST (Aspartate transaferase). Statistical significance vs. healthy control is indicated by * (p < 0.05), ** (p < 0.01), and *** (p < 0.001). Statistical significance vs. diabetic control is indicated by $ (p < 0.05), $$ (p < 0.01), and $$$ (p < 0.001). ns = p > 0.05.*

The mean red blood cell levels of MDA and serum levels of NO of diabetic rats treated by OLE were 0.173±0.026 mmol/g and 5.32±0.69 µmol/l, respectively (P<0.05). Also, in diabetic rats treated by OLE/ZnO-NPs, very significant decreases in the latter parameters were observed (0.132±0.018mmol/g and 3.89±0.78 µmol/l, respectively; *P*<0.001) when compared to those of the untreated diabetic rats (0.287±0.103 mmol/g and 6.98±1.25 µmol/l, respectively).On the other hand, the mean plasma activity of catalase (CAT) and GSH levels were very significantly increased in OLE-treated diabetic rats when compared to those of the untreated diabetic rats (0.063±0.011 U/g protein, and .26±0.34 mmol/g, respectively; p<0.05). While, SOD, as well as those of TAC levels were extremely significantly increased in OLE-treated diabetic rats (33.71±4.01%inhibiton, 10.42±1.12 mmol/g, *p*<0.001). Also, in diabetic rats which were treated with OLE/ZnO-NPs the values of these four markers were 0.078±0.013 U/g protein, 2.16±0.63 mmol/g and11.59±0.71 mmol/l, 38.3±3.04 %inhibition as well as respectively; *p*<0.001) when compared to that of the diabetic untreated rats (0.031±0.013 U/g protein, 7.42±1.05 mmol/l, and 19.2±2 %inhibition, respectively; table 4).

Table 4 Antioxidant assays in control, diabetic and treated groups.

Variables	MDA *(mmol/g)*	NO *(µmol/l)*	GSH *(mmol/g)*	CAT *(U/g protein)*	TAC *(mmol/l)*	SOD *(%inhibition)*
G1	0.085±0.014	2.79±1.19	5.09±0.83	0.129±0.03	13.03±0.85	43.03±4.59
G2	0.287±0.103***	6.98±1.25***	2.16±0.63***	0.031±0.013***	7.42±1.05***	19.2±2***
G3	0.230±0.062**	5.88±0.53***	2.84±0.34***	0.07±0.02***	10.13±0.47$^{***, \$\$\$}$	30.48±3.44$^{***, \$\$\$}$
G4	0.173±0.026$^{ns, \$}$	5.32±0.69$^{***, \$}$	3.26±0.34$^{***, \$}$	0.063±0.011$^{***, \$}$	10.42±1.12$^{***, \$\$\$}$	33.71±4.01$^{**, \$\$\$}$
G5	0.132±0.018$^{\$\$\$}$	3.89±0.78$^{ns, \$\$\$}$	3.57±0.35$^{***, \$\$\$}$	0.078±0.013$^{***, \$\$\$}$	11.59±0.71$^{**, \$\$\$}$	38.3±3.04$^{ns, \$\$\$}$

*G1 (healthy control group), G2 (Diabetic control group), G3 (Sc-insulin-treated group), G4 (Oral OLE-treated group), G5 (I.P OLE/ZnO-NPs-treated group). GSH (reduced glutathione), NO (nitric acid), MDA (malondialdehyde), CAT (catalase), SOD (superoxide diamutase), TAC (total antioxidants). Statistical significance vs. healthy control is indicated by * (p < 0.05), ** (p < 0.01), and *** (p < 0.001). Statistical significance vs. diabetic control is indicated by $ (p < 0.05), $$ (p < 0.01), and $$$ (p < 0.001). ns = p > 0.05.*

Liver glycogen

Fig. 5 illustrates the histopathology of liver sections stained with PAS among different experimental groups. In the control group, **Fig. 5C** showed uniform distribution of PAS positivity in the cytoplasm of hepatocytes surrounding the central vein (CV), sinusoid (S), nucleus(N), and hepatocytes (H) (PAS, 400X). In contrast, in the diabetic group (**fig. 5DM**), the staining showed uniform PAS positivity reaction in the cytoplasm of hepatocytes surrounding CV, congested central vein (CCV), and H(PAS, 400X). The insulin-treated group (**fig. 5INS**) demonstrated restoration of the glycogen distribution in the hepatocytes radiating from CV, H, N, and S: sinusoid (PAS, 400X). Similarly, in the OLE-treated group **(fig. 4ext)**, the glycogen distribution was restored in the hepatocytes radiating from

CV, H, S, N (PAS, 400X). Notably, OLE/ZnO-NPs-treated group (**fig. 5ZnO**) exhibited moderate restoration of the glycogen distribution in the hepatocytes radiating from CV, CCV, H, N, and S (PAS, 400X). The mean glycogen levels were calculated from PAS staining, and the results were depicted in **fig. 5A**. In this regard, it was observed that the hepatic tissue's glycogen contents were significantly lower (p<0.001) in rats with STZ-induced diabetes versus those of the untreated control (6.23±1.6 mg/g tissue). After treatment with OLE and OLE/ZnO-NPs, the diabetic rats noted a remarkable increase in their liver glycogen contents (3.48±0.55 and 2.96±0.9 mg/g tissue, respectively; p<0.001 and p<0.05), if compared with that of the diabetic control (1.7±0.46 mg/g tissue).

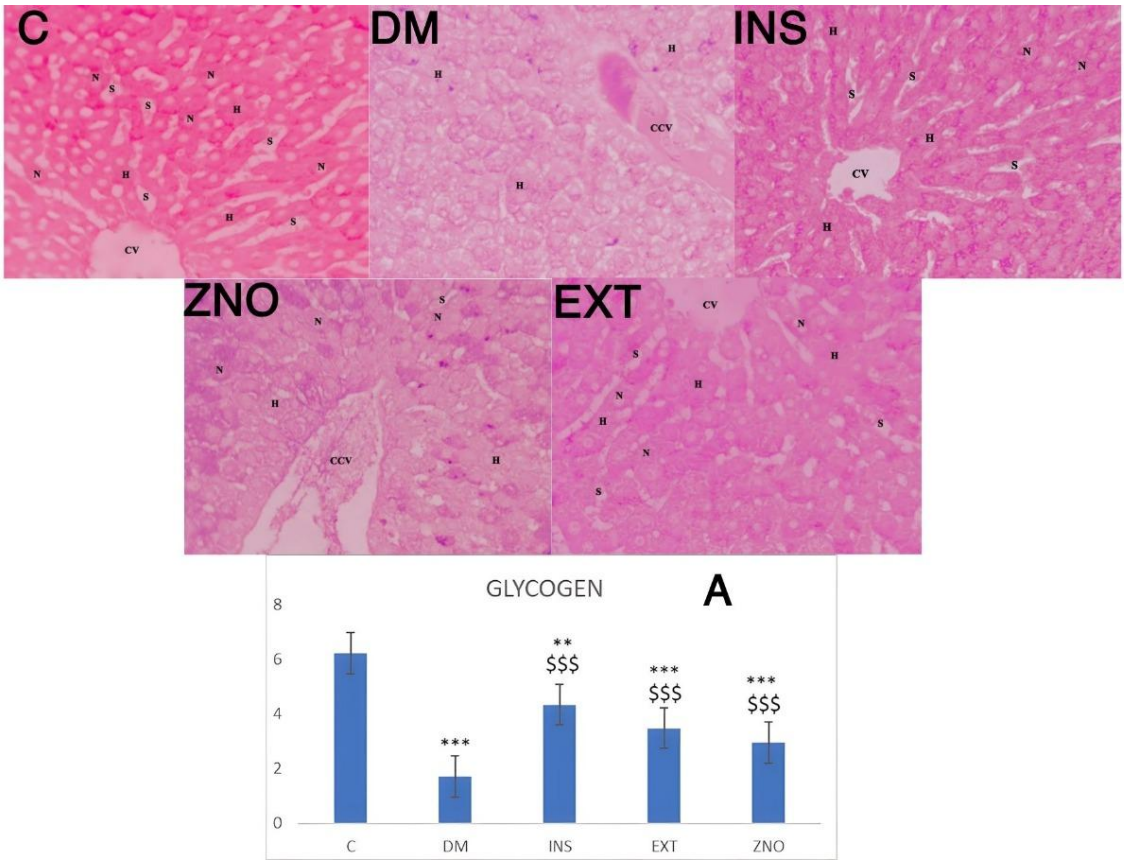

Figure 5 Histopathology of liver sections stained with PAS and its quantitative analysis of PAS staining intensity. *C: Photomicrograph of control group. DM (Diabetic control group), INS (Sc-insulin treated group), EXT (Oral* OLE*-treated group), ZnO (i.p.* OLE/ZnO-NPs*-treated group). H: hepatocytes, N: nucleus and S: sinusoid (PAS, 400X). Statistical significance vs. healthy control is indicated by * (p < 0.05), ** (p < 0.01), and *** (p < 0.001). Statistical significance vs. diabetic control is indicated by $ (p < 0.05), $$ (p < 0.01), and $$$ (p < 0.001). ns = p > 0.05.*

Histopathological changes in liver, kidneys and pancreatic tissues

Fig. 6 A illustrates the histopathological changes in liver sections among different experimental groups. In the control group **(G1)**, the liver exhibited normal hepatic architecture characterized by a clearly defined central vein, well-organized hepatocyte with distinct nuclei, intact blood sinusoids, and normally distributed Kupffer cells. In contrast, the diabetic group **(G2)** revealed marked hepatic damage, including a congested central vein (CCV), loss of hepatocytes boundaries, vacuolated hepatocytes, hemorrhage between hepatocytes, and inflammatory cell infiltration. The insulin-treated group **(G3)** demonstrated partial restoration of hepatic architecture with CCV, hepatocytes, and distinct nuclei comparable to those of normal, although severe hemorrhage between hepatocytes and within sinusoids was still evident. Notably, the OLE-treated group (**G4**) exhibited a more pronounced restoration of normal hepatic architecture, with well-defined congested central vein, hepatocytes, sinusoids, and nuclei. However, only a slight hemorrhage between hepatocytes was observed. The OLE/ZnO-NPs group (**G5**) exhibited slight improvement towards normal architecture with the presence of CCV, hepatocytes, sinusoids, and nuclei. However, hemorrhage and inflammatory cell infiltration persisted.

Fig. 6 B illustrates the histopathological findings of kidney sections among different experimental groups. The control group in **(fig. 6BG1)**, the kidney exhibited normal renal architecture, which was characterized by normal glomeruli, normal Bowmen's space, and normal renal tubules. Conversely, the diabetic group of rats revealed marked renal damage, including glomerular atrophy, widened Bowmen's space, and damaged renal tubules. Severe interstitial hemorrhage, interstitial infiltration, degenerated renal tubules, and necrosis (*) of renal architecture were also detected **(fig. 6BG2)**. The insulin-treated groups (**fig. 6BG3**) demonstrated restoration of normal renal architecture with normal glomeruli, normal Bowmen's space, and normal renal tubules. Although severe interstitial and around glomerular inflammatory cells infiltration was still evident. Similarly, a slight improvement towards normal renal architecture with slightly atrophied glomeruli, Bowmen's space, some normal renal tubules and others are degenerated. Severe interstitial inflammatory cell infiltration persisted in the OLE-treated group **(fig. 6BG4)**. The OLE/ZnO-NPs-treated group showed slightly normal renal architecture with normal glomeruli, normal Bowmen's space, and damaged renal tubules. Interstitial hemorrhage, interstitial infiltration, and necrosis (*) of renal architecture are observed **(fig. 6BG5)**.

In **fig. 6 C**, the control displayed normal pancreatic architecture with well-organized pancreatic acini and thin connective tissue septae (**fig. 6CG1**). In contrast, the diabetic group (**fig. 6CG2**) exhibited severe pancreatic damage, characterized by disorganized architecture, widening of connective tissue septae, hemorrhage, and dense inflammatory cell infiltration. Treatment with insulin (**fig. 6CG3**) markedly restored the normal pancreatic structure, with preservation of acini and septae and a reduction in pathological alterations. Similarly, the OLE-treated group (**fig. 6CG4**) showed restoration of normal pancreatic architecture, with clearly defined acini and thin connective tissue septae approaching that of the control group. Although a slight hemorrhage was still evident. The OLE/ZnO-NPs-treated group (**fig. 6CG5**) exhibited a slight restoration of normal pancreatic architecture with clearly defined acini, thin connective tissue septae, and minimal hemorrhage was still observed.

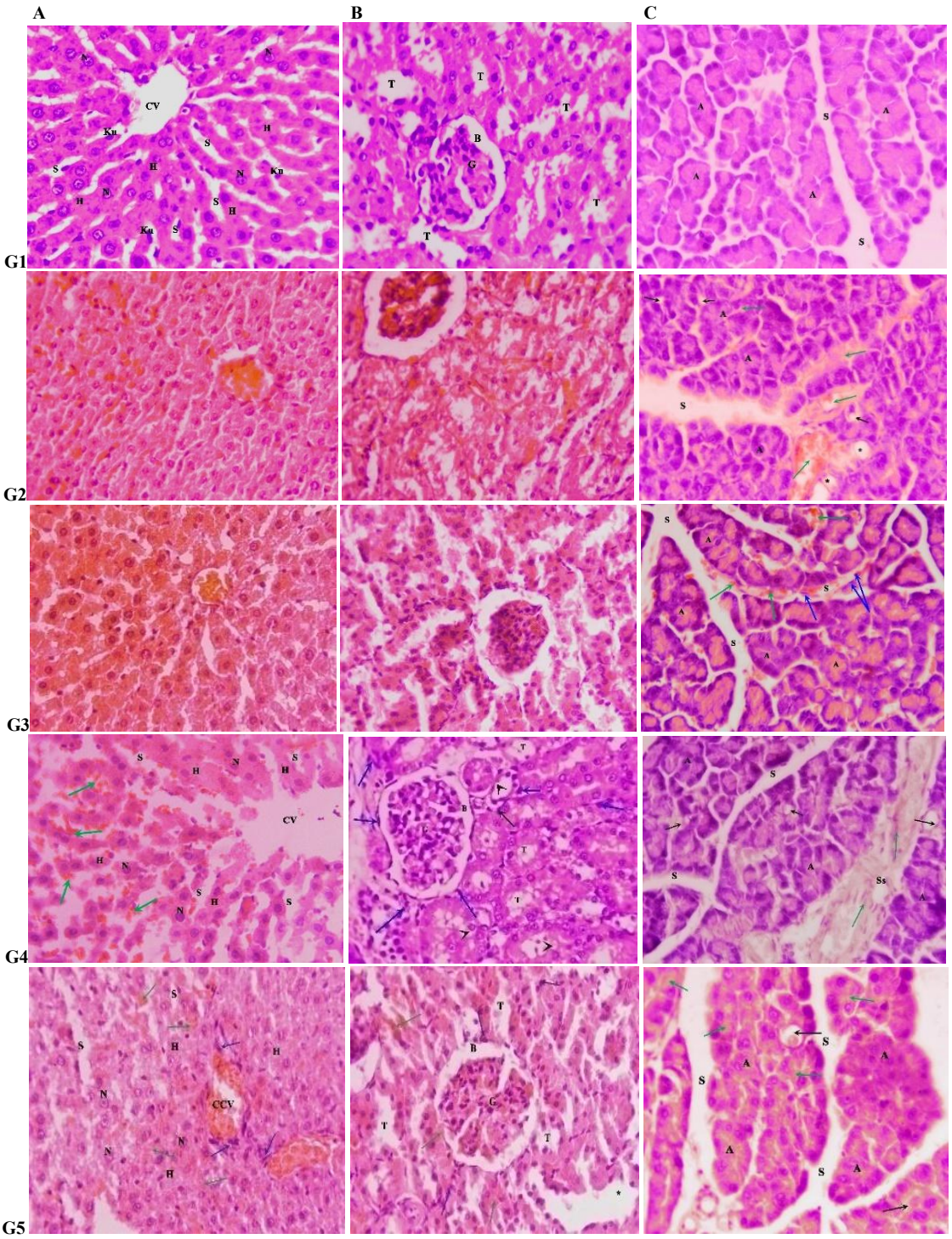

Figure 6 Tissue pathology. Histopathological findings of liver (A), histopathological findings of kidney (B) and histopathology of pancreas (C). *(G1) Photomicrograph of control group. (G2) Photomicrograph of diabetic group. (G3) Photomicrograph of insulin-treated group. (G4) Photomicrograph of OLE-treated group. (G5) Photomicrograph of OLE/ZnO-NPs -treated group. S indicates widened connective tissue septae, necrosis*, hemorrhage (green arrow) and vacuolated acini (black arrow). pancreatic acini (A), thin connective tissue septae (S), and inflammatory cells infiltration (blue arrow)*

Erythrocytes glucose uptake in hyperglycemic conditions with and without the addition of OLE and OLE/ZnO-NPs

After incubation of erythrocytes of the healthy control and diabetic rats in hyperglycemic PBS at 37°C for 2 hours with and without addition of 25 µl, 50 µl and 100 µl of OLE and OLE/ZnO-NPs, the % of glucose uptake in erythrocytes of all diabetes-induced rats was decreased compared to that of the control. Conversely, when OLE and OLE/ZnO-NPs were added, the erythrocytes' glucose uptakes were higher than when they were not (**fig. 7**).

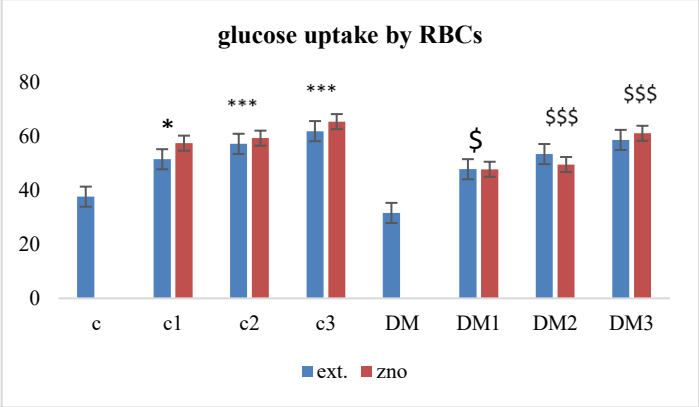

Figure 7 % Glucose uptake by red blood cells (RBCs) of controls and diabetic rats, with and without the addition of OLE, OLE/ZnO-NPs. *C: RBCs of control rat, c1: RBCs of control+25µl of OLE or OLE/ZnO-NPs, c2: RBCs of control rat+50µl of OLE or OLE/ZnO-NPs, c3: RBCs of control+ 100µl of OLE or OLE/ZnO-NPs, DM: RBCs of diabetic rat, DM1: RBCs of diabetic rat+25µl of OLE or OLE/ZnO-NPs, DM2: RBCs of diabetic rat+50µl of OLE or OLE/ZnO-NPs comparing, DM3: RBCs of diabetic rat+100µl of OLE or OLE/ZnO-NP.*s Statistical significance vs. healthy control is indicated by * ($p < 0.05$), ** ($p < 0.01$), and *** ($p < 0.001$). Statistical significance vs. diabetic control is indicated by $ ($p < 0.05$), $$ ($p < 0.01$), and $$$ ($p < 0.001$). ns = $p > 0.05$.

Table 5's findings demonstrated that the FBG level was negatively and significantly correlated with ADP, CAT, TAC, SOD, and GSH but positively and significantly correlated with insulin level, HOMA-IR, leptin, HbA1c, LAR, MDA, and NO. Also. LAR was negatively correlated with serum ADP levels but positively correlated with serum leptin levels.

Table 5 Values of the correlation's coefficients between the individual values of fasting blood gucose (FBG), insulin, HOMA-IR, adiponectin (ADP), leptin, adiponectin /leptin (A/L) ratio and leptin/ adiponectin ratio (LAR) with each other's and with antioxidants.

variables	FBG (mmol/l	Insulin (µIU/mL)	HOMA-IR	ADP (ng/ml)	Leptin (ng/ml)	A/L	LAR
FBG							
r	1	0.458	0.815	-0.671	0.673	-0.581	0.625
P		<0.01	<0.001	<0.001	<0.001	<0.001	<0.001
Insulin							
r	0.458	1	0.801	-0.548	0.618	-0.542	0.533
P	<0.01		<0.001	<0.001	<0.001	<0.001	<0.001
HOMA-IR							
r	0.815	0.801	1	-0.606	0.749	-0.531	0.681
P	<0.001	<0.001		<0.001	<0.001	<0.001	<0.001
ADP							
r	-0.671	-0.548	-0.606	1	-0.629	0.945	-0.682
P	<0.001	<0.001	<0.001		<0.001	<0.001	<0.001
Leptin							
r	0.673	0.618	0.749	-0.629	1	-0.554	0.729
P	<0.001	<0.001	<0.001	<0.001		<0.001	<0.001
A/L							
r	-0.581	-0.542	-0.531	0.945	-0.554	1	-0.483
P	<0.001	<0.001	<0.001	<0.001	<0.001		<0.01
HbA1c							
r	0.938	0.391	0.796	-0.654	0.687	-0.557	0.613
P	<0.001	<0.05	<0.001	<0.001	<0.001	<0.001	<0.001
CAT							
r	-0.709	-0.733	-0.780	0.751	-0.680	0.677	-0.646
P	<0.001	<0.001	<0.001	<0.001	<0.001	<0.001	<0.001
TAC							
r	-0.728	-0.705	-0.843	0.620	-0.811	0.537	-0.761
P	<0.001	<0.001	<0.001	<0.001	<0.001	<0.001	<0.001
SOD							
r	-0.677	-0.626	-0.791	0.512	-0.782	0.432	-0.701
P	<0.001	<0.001	<0.001	0.001	<0.001	<0.01	<0.001
MDA							
r	0.546	0.437	0.504	-0.501	0.667	-0.441	0.621
P	<0.001	<0.01	0.001	0.001	<0.001	<0.01	<0.001
NO							
r	0.636	0.664	0.736	-0.508	0.672	-0.424	0.663
P	<0.001	<0.001	<0.001	0.001	<0.001	<0.01	<0.001
GSH							
r	-0.706	-0.645	-0.745	0.667	-0.647	0.690	-0.526
P	<0.001	<0.001	<0.001	<0.001	<0.001	<0.001	<0.001

-r=Pearson correlation coefficient *-P= Probability*

-GSH (reduced glutathione), NO (nitric acid), MDA (malondialdehyde), CAT (catalase), SOD (superoxide diamutase), TAC (total antioxida nts capacity)

DISCUSSION

Plant-derived polyphenols have been widely investigated for their potential role in managing type 2 diabetes (T2D). In the present study, HPLC analysis confirmed the presence of multiple phenolic and flavonoid constituents in olive leaf extract (OLE), with oleuropein identified as the predominant compound. This finding is consistent with previous reports and suggests a potential contribution of this compound to the observed biological activity. The antidiabetic effects of OLE may be attributed to the combined action of its bioactive constituents. These effects may be mediated, in part, by antioxidant activity, particularly through free radical scavenging (**Haruni *et al.* 2025**), as well as by modulation of inflammatory pathways and improvement in insulin sensitivity. Polyphenols have also been reported to influence glucose metabolism through effects on carbohydrate digestion, glucose transport, and gut microbiota composition **(Shahidi and Danielski 2024)**. However, these mechanisms remain incompletely understood and may vary depending on extract composition and biological context. Furthermore, synergistic interactions among phytochemical constituents may enhance the overall biological activity of OLE, although this requires further

investigation. The predominance of oleuropein in the current study aligns with previous findings (**Cho *et al.* 2020**), while the efficiency of methanol as an extraction solvent for recovering oleuropein is also well documented (**Bouaziz *et al.* 2008**).

In addition, the phytochemical composition of OLE may contribute to the green synthesis of ZnO nanoparticles by acting as reducing and stabilizing agents (**Keshu *et al.* 2021**). The formation of OLE-mediated ZnO nanoparticles was confirmed by the appearance of a white precipitate and a characteristic UV–Vis absorption peak within the typical range reported for ZnO nanoparticles. The observed spectral behavior is consistent with previous studies, which reported similar absorption features for ZnO nanoparticles synthesized using plant extracts. Variations in peak position among different studies may be attributed to differences in particle size, synthesis conditions, and extract composition. **Ghaffar *et al.* (2023)** observed a peak at around 382 nm when ZnO was synthesized using olive fruit extract. An absorption peak at 370 nm was observed, a characteristic band of pure zinc oxide as reported by **Issam *et al.* (2021).** When ZnO NPs were produced using olive plant extract, they showed absorbance at 300 nm in the UV spectrum zone (**Alrubaie and Kadhim 2019**). Previous research has identified peaks at wavelengths 289-385 nm as the SPR of ZnO NPs (**Pachaiappan *et al.* 2021; Al-darwesh *et al.* 2024).**

FT-IR analysis further confirmed the involvement of OLE phytochemicals in nanoparticle synthesis. This observation is associated with the previously reported results of ZnO-NPs production utilizing olive leaf extract (**Awwad *et al.* 2014; Issam *et al.* 2021**). The presence of characteristic functional groups suggests that phenolic and flavonoid compounds may act as both reducing and capping agents during the formation of ZnO nanoparticles. The similarity between the FT-IR spectra of the extract and the synthesized nanoparticles indicates successful surface interaction between phytochemicals and ZnO particles. The proposed mechanism involves the interaction of hydroxyl groups of phenolic compounds (e.g., oleuropein) with Zn^{2+} ions, which forms a white milky precipitate known as $Zn(OH)_2$. This intermediate product was dried at 70°C in an air-drying oven to produce ZnO-NPs (**Ghaffar *et al.* 2023**).

Morphological analysis by TEM revealed the successful synthesis of predominantly spherical ZnO nanoparticles with an average size of 15-40 nm. Similar to **Hashemi *et al.* (2016)**, who demonstrated that TEM images revealed ZnO-NPs were spherical with an average size of 41 nm. These findings disagree with previous reports utilising olive-derived extracts, although variations in particle size reported in the literature may be attributed to differences in preparation methods and extract composition. For example, **Algarni *et al.* (2022)** demonstrated that ZnO-NPs have smooth surfaces and a size range of 86-170 nm. Generally, the reduced particle size facilitates enhanced systemic distribution and more efficient interaction with target cellular membranes.

The zeta potential is an important indicator of the colloidal stability of nanoparticles. In the present study, OLE/ZnO-NPs exhibited a negative surface charge of approximately −15.58 ± 4.49 mV, indicating moderate electrostatic stability. The average Zeta distribution size for OLE/ZnO-NPs was 473.2 nm. Comparable findings have been reported in previous studies; **Naser *et al.* (2020)** effectively synthesized ZnO with a zeta potential of -26.53 mV in de-ionized water using pulsed laser ablation on pure metal targets. Our results confirm those obtained by **Mohammadi *et al.* (2025)** at least in part on the level of potential size, who demonstrated that zinc oxide nanoparticles fabricated using Punica granatum fruit peel extract have a surface charge of -17.6 mV and an average diameter of 269.5 nm. On the contrary, greenly synthesized ZnO-NPs utilizing Padinapavonica extract show a positive zeta potential of 11.0 mV, as reported by **Alprol *et al.* (2024)**. To our knowledge, the negative surface charge reduces the interaction of nanoparticles and blood cells. These render the particles to move faster in the blood toward their target. Further, the zeta distribution of the formed NPs will have a higher hydrodynamic volume due to solvent effects in the hydrated state, as previously described by **Huang *et al.* (2010)**.

The polydispersity index (PDI = 0.0326) indicates a highly homogeneous nanoparticle distribution (0–1), suggesting good dispersion stability. It is well established that nanoparticle size, stability, and morphology are strongly influenced by synthesis conditions, reaction kinetics, and the nature of stabilizing agents present in the extract (**Danaei *et al.*, 2018; Narayanan *et al.*, 2020**). Overall, the combination of low PDI and moderate negative zeta potential suggests relatively stable colloidal behavior of the synthesized OLE/ZnO-NPs, which may help maintain dispersion in biological media and reduce aggregation. Such stability is important as nanoparticle aggregation can reduce surface area and potentially affect biological activity (**El-Zahed *et al.* 2021**). The stability of these nanoparticles can be attributed to the role of OLE phytochemicals, which may act as capping agents by adsorbing onto the nanoparticle surface during synthesis. This adsorption can provide steric and electrostatic stabilization, thereby limiting particle growth and aggregation and contributing to controlled nanoparticle formation (**Fayed *et al.* 2025**).

Hyperglycemia-induced glucotoxicity is a key contributor to insulin resistance in T2DM. In the present study, the diabetic model demonstrated clear features of impaired glucose homeostasis and insulin resistance, as reflected by alterations in glycemic and insulin-related indices. Treatment with OLE, OLE/ZnO-NPs, and insulin resulted in marked improvement in these parameters, suggesting enhanced insulin sensitivity and overall glycemic control. The observed antidiabetic effects of OLE/ZnO-NPs may be attributed to multiple mechanisms. These may include improved peripheral glucose utilization, modulation of insulin signaling pathways, and possible enhancement of pancreatic β-cell function. The current findings are consistent with previous reports demonstrating the efficacy of plant-mediated ZnO nanoparticles and polyphenol-rich extracts in ameliorating insulin resistance (**Ahmed *et al.*, 2022; Qadir *et al.*, 2016**). Moreover, improved glucose tolerance was supported by the oral glucose tolerance test (OGTT) response, including a reduction in the overall glycemic exposure as reflected by the area under the curve (AUC). This effect may be mediated, at least in part, through inhibition of intestinal carbohydrate-digesting enzymes, enhanced hepatic glucose uptake and storage, and/or improved glucose-stimulated insulin secretion (GSIS). However, these mechanisms remain to be fully elucidated and may depend on both nanoparticle characteristics and extract composition (**Umrani and Paknikar, 2014**).

Zinc plays an important role in metabolic regulation, including lipid metabolism and inflammatory processes, which are closely linked to T2DM and its complications. In the present study, treatment with OLE and OLE/ZnO-NPs modulated adipokine profiles, as evidenced by reduced leptin levels and increased adiponectin levels compared to untreated diabetic rats. This shift suggests a potential improvement in insulin sensitivity, as the leptin-to-adiponectin ratio (LAR) is considered a reliable marker of insulin resistance. The observed correlations between LAR, leptin, and adiponectin further support this relationship and are consistent with previous reports (**Osama *et al.*, 2024; Al-Hamodi *et al.*, 2014).** In addition, diabetic animals exhibited dyslipidemia, a common feature associated with insulin resistance. Treatment with OLE/ZnO-NPs improved the lipid profile, indicating a potential antihyperlipidemic effect. This improvement may be linked to enhanced lipid metabolism, possibly through increased fatty acid oxidation and reduced lipogenesis, although these mechanisms require further clarification. Similar findings have been reported for ZnO nanoparticle-based therapies in diabetic models (**Ahmed *et al.*, 2022; John *et al.*, 2020**). Also, Treatment with insulin lowered TC, TG, and LDL levels while increasing HDL in diabetic rats. These findings are consistent with **Hassanien *et al.* (2020).**

Markers of liver function also suggested hepatic impairment in diabetic rats, while treatment with OLE/ZnO-NPs improved these alterations, indicating a potential hepatoprotective effect. This may be attributed to improved metabolic control and reduced oxidative stress, as supported by previous studies (**Hassanien *et al.*, 2020; Ahmed *et al.*, 2022).** However, it should be noted that the effects of ZnO nanoparticles on liver function may vary depending on dose and particle characteristics. Renal function markers were also affected in diabetic conditions, reflecting the progression of metabolic disturbances. Treatment with OLE, OLE/ZnO-NPs, and insulin appeared to improve these parameters, which may suggest a protective effect against diabetic nephropathy. This effect could be related to improved glycemic control and antioxidant activity (**Afify *et al.*, 2018).** These compounds' hypoglycemic activity may be due to two mechanisms: (a) potentiation of glucose-induced insulin release and (b) enhanced peripheral glucose absorption (**Eidi *et al.* 2009).** Another way by which OLE may exert its hypoglycemic impact is by inhibiting pancreatic amylase activity. Further, OLE may also block starch digestion and glucose uptake, or stimulate hepatic glycogen production, resulting in reduced hyperglycemia (**Afify *et al.* 2018**).

Oxidative stress plays a central role in the pathogenesis of T2DM and its complications. In the present study, diabetic conditions were associated with increased lipid peroxidation and impaired antioxidant systems. Treatment with OLE/ZnO-NPs improved antioxidant status, as indicated by enhanced activity of endogenous antioxidant enzymes. These findings suggest that the therapeutic effects of OLE/ZnO-NPs may be partially mediated through attenuation of oxidative stress, in agreement with previous reports (**Ahmed *et al.*, 2022; Umrani and Paknikar, 2014**). The observed increase in erythrocyte glucose uptake *in vitro* may reflect an improvement in membrane glucose transport efficiency, likely mediated by enhanced GLUT1 activity and reduced oxidative stress. Although erythrocyte glucose transport is insulin-independent **(Maritim *et al.*, 2003)**, this finding may serve as a supportive indicator of improved systemic glucose handling, which is consistent with the observed *in vivo* improvements in glycemic control, lipid profile, and insulin sensitivity (**Szabó *et al.*, 2021**). These effects may be attributed, at least in part, to the antioxidant properties of OLE and OLE/ZnO-NPs, likely due to their phenolic and flavonoid constituents. Similar improvements in erythrocyte glucose uptake following treatment with plant-derived extracts have been previously reported (**Mahdy *et al.*, 2017; Eldebsy *et al.*, 2026**).

In addition, hepatic glycogen content, which is typically reduced under diabetic conditions due to impaired insulin action, appeared to improve following treatment. This suggests a potential restoration of hepatic glucose storage capacity and improved glucose utilization, consistent with previous findings using OLE in diabetic models (**AbdRabou *et al.*, 2024**). Furthermore, the relationship between adipokines and insulin resistance was supported by correlation analysis, where LAR showed a positive association with leptin and HOMA-IR, and a negative association with adiponectin. The potential value of LAR as an indicator of insulin resistance and metabolic risk in T2DM. These findings were similar to the studies of **Al-Hamodi *et al.* (2014)** and **Agostinis-Sobrinho *et al.* (2022)**.

Overall, the findings of the present study suggest that OLE and OLE/ZnO-NPs exhibit promising antidiabetic potential through multifactorial mechanisms. These include improvement of glycemic control, modulation of insulin sensitivity, regulation of lipid metabolism, and attenuation of oxidative stress. The integration

of phytochemicals within ZnO nanoparticles may enhance their biological activity, possibly through improved stability and bioavailability. Importantly, the observed effects across metabolic, biochemical, and oxidative stress parameters indicate a coordinated therapeutic response rather than a single-target action. However, despite these encouraging findings, the exact molecular mechanisms underlying these effects remain to be fully elucidated. In addition, further studies are required to evaluate long-term safety, optimal dosing, and potential clinical applicability.

CONCLUSION

The present study demonstrated that the methanolic extract of Olea europaea leaves and its ZnO nanoparticle formulation exerted significant antidiabetic and antioxidant effects in STZ-induced diabetic rats. Both treatments improved glycemic control, enhanced glycogen content, ameliorated dyslipidemia, and reduced oxidative stress while preserving pancreatic histoarchitecture. In addition, they modulated adipokines, improving adiponectin and leptin levels and restoring the leptin/adiponectin ratio. Notably, the nano-formulated group (G5) showed the most pronounced beneficial effects compared to the extract group (G4), indicating enhanced therapeutic efficacy of the nano-formulation. These findings suggest that olive leaf bioactive compounds, particularly in nano-delivered form, may serve as promising natural agents for diabetes management through modulation of insulin sensitivity, oxidative stress, and metabolic homeostasis.

Acknowledgements: The authors would like to dedicate this work to the memory of prof. Elshahat A. Toson, who passed away before the publication of this manuscript.

CRediT authorship contribution statement: Elshahat A. Toson conceptualized the entire work, contributions in writing the manuscript and interpretation of data and revised the manuscript. With Hadeer A. Omar, Elshahat A. Toson prepared the first draft of the manuscript, its rewriting and data interpretation. Entsar A. Saad, supervision, participation in data collection, and final revision. By Hadeer A. Omar collects data; experimental work and data analysis were done. Hadeer A. Omar and Entsar A. Saad read and approved the final paper.

Declaration of competing interest: The authors declare that there is no conflict of interests regarding the publication of this paper.

Data availability: All data generated or analyzed during this study are included in this manuscript.

Formatting of funding sources: This research received no specific grant from any funding agency in the public, commercial, or not-for-profit sectors.

Ethical approval: All animal experiments are carried out according to the Guide for the Care and Use of Laboratory Animals, according to the IACUC. approved by the Institutional Review Board of the Faculty of Medicine (DFM-IRB 00012367-25-07-022).

REFERENCES

AbdRabou, M.A.A., Massoud, D., Asran, A.M., Alrayes, Z.R. , Al-Otaibi, A.M., Alghamdi, F.A., Germoush, M.O., Alruwaili, H.K. , Nabeeh, A., Mehany, A.B.M., 2024. Therapeutic Effect of Mesenchymal Stem Cells and Olive Leaf Extract Against Cytotoxicity Induced by Streptozotocin in Gestational Diabetes Rats. *Cellular Physiology and Biochemistry*. 58(6), 702–721. https://doi.org/10.33594/000000744

Abugomaa, A., Elbadawy, M., 2020. Olive leaf extract modulates glycerol-induced kidney and liver damage in rats. *Environmental Science and Pollution Research*. 27(17), 22100–22111. https://doi.org/10.1007/s11356-020-08371-6

Afify, AE.M.R., El-Beltagi, H.S., Fayed, S.A., El-Ansary, A.E., 2018. Beneficial and potent effect of olive leaves extract on hyperglycemic state, kidney and liver function in STZ-induced type 2 diabetes mellitus. *Fresenius Environmental Bulletin.* 27, 3733–3739.

Agostinis-Sobrinho, C., Vicente, S., Norkiene, S., Rauckienė-Michaelsson, A., Kievisienė, J., Dubey, Arturas, R.V.P., Lopes, L., Santos, R., 2022. Is the Leptin/Adiponectin Ratio a Better Diagnostic Biomarker for Insulin Resistance than Leptin or Adiponectin Alone in Adolescents? *Children*. 9(8), 1193. https://doi.org/10.3390/children9081193.

Ahmed, E.S.A., Mohamed, H.E., Farrag, M.A., 2022. Luteolin loaded on zinc oxide nanoparticles ameliorates non-alcoholic fatty liver disease associated with insulin resistance in diabetic rats via regulation of PI3K/AKT/FoxO1 pathway. *International Journal of Immunopathology and Pharmacology*. 36(1), 3946320221137435. https://doi.org/10.1177/03946320221137435

Al-Attar, A. M., & Alsalmi, F. A., 2019. Effect of Olea europaea leaves extract on streptozotocin induced diabetes in male albino rats. *Saudi Journal of Biological Sciences*, 26(1), 118–128. https://doi.org/10.1016/j.sjbs.2017.03.002

Al-darwesh, M.Y., Ibrahim, S.S., Mohammed, M.A., 2024. A review on plant extract mediated green synthesis of zinc oxide nanoparticles and their biomedical applications. *Results in Chemistry*. 7, 101368. https://doi.org/10.1016/j.rechem.2024.101368

Algarni, T.S., Abduh, N.A.Y., Aouissi, A., and Al Kahtan, A., 2022. Photodegradation of methyl orange under solar irradiation on Fe-doped ZnO nanoparticles synthesized using wild olive leaf extract. *Green Processing and Synthesis*. 11(1), 895–906. https://doi.org/10.1515/gps-2022-0077

Al-Hamodi, Z., Al-Habori, M., Al-Meeri, A., and Saif-Ali, R., 2014. Association of adipokines, leptin/adiponectin ratio and C-reactive protein with obesity and type 2 diabetes mellitus. *Diabetology & Metabolic Syndrome*. 6(1), 99. https://doi.org/10.1186/1758-5996-6-99.

Alprol, A.E., Eleryan, A., Abouelwafa, A., Gad, A., Hamad, T.M., 2024. Green synthesis of zinc oxide nanoparticles using Padina pavonica extract for efficient photocatalytic removal of methylene blue. *Scientific Reports*. 14(1), 32160. https://doi.org/10.1038/s41598-024-80757-9.

Al-Rejaboo, M.A., Al-Tarjuman, J.K., Al-Dulaimi, F.K.Y., Al-Sumaidaiea, B.Z., 2025. Fungi isolated from soils adjacent to olive trees in Nineveh Governorate. *Regulatory Mechanisms in Biosystems*. 33(1), e25017. https://doi.10.15421/0225017

Alrubaie E A.A. and Kadhim R.E. 2019. Synthesis of ZnO Nanoparticles from Olive Plant Extract. Plant Archives. 19(2), 339-344.

Al-Saaidi, J. A. A., Kareem, H. M. A., aidi, A., & Al-Tameemi, W. T. M., 2014. Antihyperglycemic Effects of thymoquinone in diabetic rats. *Basrah Journal of Veterinary Research*, 13(2), 180–192. https://doi.10.33762/bvetr.2014.98809

Al-Saeed, F.A., 2023. The Protective Effects of Olive (Olea oleaster) Leaves Extract on Male Rats Exposed to Cadmium Toxicity. *Advances in Animal and Veterinary Sciences*. 11(10), 1639–1643. https://doi.org/10.17582/journal.aavs/2023/11.10.1639.1643

Arivarasan, V.K., Diwakar, D., Kamarudheen, N., Loganathan, K., 2025. Current approaches in CRISPR-Cas systems for diabetes. *Progress in Molecular Biology and Translational Science*. 210, 95–125. https://doi.org/10.1016/bs.pmbts.2024.08.002

Awwad, A., Albiss, B.L., Ahmad, A., 2014. Green Synthesis, Characterization and Optical Properties of Zinc Oxide Nanosheets Using Olea Europea Leaf Extract. *Advanced Materials Letters*. 5(9), 520–524. https://doi.org/10.5185/amlett.2014.5575

Basuny, A., Abdelaaty, L., Zakhari, C., Hussein, R.R.S., Mohamed, M.R.A., Ali, S.A.G., 2023. Efficacy of the traditional use of Olive Leaves decoction as Anti-diabetic Agent in Geriatrics. *NILES journal for Geriatric and Gerontology*. 6(2), 420–431. https://doi.org/10.21608/niles.2023.296455

Bouaziz, M., Fki, I., Jemai, H., Ayadi, M., Sayadi, S., 2008. Effect of storage on refined and husk olive oils composition: Stabilization by addition of natural antioxidants from Chemlali olive leaves. *Food Chemistry*. 108(1), 253–262. https://doi.org/10.1016/j.foodchem.2007.10.074.

Carroll, N.V., Longley, R.W., Roe, J.H., 1956. The Determination of Glycogen in Liver and Muscle by Use of Anthrone Reagent. *Journal of Biological Chemistry*. 220(2), 583–593. https://doi.org/10.1016/S0021-9258(18)65284-6.

Danaei, M., Dehghankhold, M., Ataei, S., Davarani, F.H., Javanmard, R., Dokhani, A., Khorasani, S. and Mozafari, M.R., 2018. Impact of Particle Size and Polydispersity Index on the Clinical Applications of Lipidic Nanocarrier Systems. *Pharmaceutics*. 10(2), 57. https://doi.org/10.3390/pharmaceutics10020057

Eidi, A., Eidi, M., Darzi, R., 2009. Antidiabetic Effect of Olea Europea L. Antidiabetic Effect of Olea europaea L. in Normal and Diabetic Rats. *Phytotherapy Research*. 23(3), 347–350. https://doi.org/10.1002/ptr.

Eldebsy, S.S., Saad, E.A., El Sadda, R.R., 2026. Optimized renal protection with combined thymoquinone and glycine treatment: synergistic management of streptozotocin-induced nephropathy. *Naunyn-Schmiedeberg's Archives of Pharmacology*. 399, 5621–5632. https://doi.org/10.1007/s00210-025-04725-4

Elneely, E.A., Saad, E.A., Elsharkawy, A.A., Toson, E.A., Attia, Z.R., 2025. Oxidative Stress Biomarkers and NLRP3 Polymorphism in Type 1 Diabetes. *Egyptian Journal of Chemistry*. 68(8), 363-372. https://doi.org/10.21608/ejchem.2025.327552.10618

El-Zahed, M.M., Baka, Z.A., Abou-Dobara, M.I., El-Sayed, A.K., Aboser, M.M. and Hyder, A., 2021. In vivo toxicity and antitumor activity of newly green synthesized reduced graphene oxide/silver nanocomposites. *Bioresources and Bioprocessing.* 8(1), 44. https://doi.org/10.1186/s40643-021-00400-7.

Fayed, R.M., Mohamed, B.Z.A., Farouk, B.H., Hamdy, B., 2025. Antibacterial and cytotoxic activities of a newly green synthesized ZnO/Se nanocomposite combined with Washingtonia robusta H. Wendl fruit extract. *Biocatalysis and Agricultural Biotechnology*. 64(1), 103500. https://doi.org/10.1016/j.bcab.2025.103500.

Ganesan, P., Ramalingam, P., Karthivashan, G., Ko, Y.T., Choi, D-K., 2018. Recent developments in solid lipid nanoparticle and surface-modified solid lipid nanoparticle delivery systems for oral delivery of phyto-bioactive compounds in various chronic diseases. *International Journal of Nanomedicine.* 13(15), 1569–1583. https://doi.org/10.2147/IJN.S155593.

Ghaffar, S., Abbas, A., Naeem-ul-Hassan, M., Assad, N., Sher, M., Ullah, S., Alhazmi, H.A., Najmi, A., Zoghebi, K., Al Bratty, M., Hanbashi, A., Makeen, H.A. and Amin, H.M.A., 2023. Improved Photocatalytic and Antioxidant Activity of Olive Fruit Extract-Mediated ZnO Nanoparticles. *Antioxidants*. 12(6), 1201. https://doi.org/10.3390/antiox12061201

Gnanasangeetha D. and SaralaThambavani D., 2013. One Pot Synthesis of Zinc Oxide Nanoparticles via Chemical and Green Method. Research Journal of Material Sciences. 1(7), 1-8.

Gorzynik-Debicka, M., Przychodzen, P., Cappello, F., Kuban-Jankowska, A., Marino, G.A., Knap, N., *et al.* 2018. Potential Health Benefits of Olive Oil and Plant Polyphenols. *International Journal of Molecular Sciences (IJMS)*. 19, 686. https://doi.org/10.3390/ijms19030686.

Habib, S.A., Saad, E.A., Elsharkawy, A.A., Attia, Z.R., 2015. Pro-inflammatory adipocytokines, oxidative stress, insulin, Zn and Cu: Interrelations with obesity in Egyptian non-diabetic obese children and adolescents. *Advances in Medical Sciences*. 60(2), 179-185. https://doi.org/10.1016/j.advms.2015.02.002

Haruni, M.d.J., Parvin, M.S., Munira, S., Islam, M.d.E., 2025. Phytochemical Profile and Evaluation of the Antioxidant, Anticancer, and Antimicrobial Potential of *Artocarpus lacucha* Bark Extracts: In Vitro and In Silico Studies. *Journal of Food Biochemistry*. 2025, 17. https://doi.org/10.1155/jfbc/8016598.

Hashemi, S., Asrar, Z., Pourseyedi, S., Nadernejad, N., 2016. Green synthesis of ZnO nanoparticles by Olive (Olea europaea). *IET Nanobiotechnology*. 10(6), 400–404. https://doi.org/10.1049/iet-nbt.2015.0117

Hassanien, M.M., Saad, E.A., Radwan, K.H., 2020. Antidiabetic activity of cobalt–quercetin complex: A new potential candidate for diabetes treatment. *Journal of Applied Pharmaceutical Science*. 10(12), 044-052. https://doi.org/10.7324/JAPS.2020.101206

Huang, N.M., Lim, H.N., Radiman, S., Khiew, P., Chiu, W.S., Hashim, R., Chia, C-h., 2010. Sucrose ester micellar-mediated synthesis of Ag nanoparticles and the antibacterial properties. *Colloids and Surfaces A: Physicochemical and Engineering Aspects.* 353(1), 69–76. https://doi.org/10.1016/j.colsurfa.2009.10.023.

Hui, H., Ma, W., Cui, J., Gong, M., Wang, Y., Zhang, Y., He, T., Bi, Y., He, Y., 2017. Periodic acid-Schiff staining method for function detection of liver cells is affected by 2% horse serum in induction medium. *Molecular Medicine Reports*. 16(6), 8062–8068. https://doi.org/10.3892/mmr.2017.7587

Cho, W-Y., Kim, D-H., Lee, H-J., Yeon, S-J., and Lee, C-H., 2020. Evaluation of Effect of Extraction Solvent on Selected Properties of Olive Leaf Extract. *Journal of Food Quality*. 2020(11), 1–7. https://doi.org/10.1155/2020/3013649

Iantomasi, M., Terzo, M., Tsiani, E., 2024. Anti-Diabetic Effects of Oleuropein. *Metabolites*. 14(11), 581. https://doi.org/10.3390/metabo14110581

Issam, N., Naceur, D., Nechi, G., Maatalah, S., Zribi, K., Mhadhbi, H., Naceur, D.E., 2021. Green synthesised ZnO nanoparticles mediated by Olea europaea leaf extract and their antifungal activity against *Botrytis cinerea* infecting faba bean plants. *Archives of Phytopathology and Plant Protection*. 54, 1083–1105. https://doi.org/10.1080/03235408.2021.1889859

Jain, S.K., 1989. Hyperglycemia can cause membrane lipid peroxidation and osmotic fragility in human red blood cells. *Journal of Biological Chemistry*. 264(35), 21340–21345. https://doi.org/10.1016/s0021-9258(19)30085-7

John, A.D., Ragavee, A., Selvaraj, A.D., 2020. Protective role of biosynthesised zinc oxide nanoparticles on pancreatic beta cells: an in vitro and in vivo approach. *IET Nanobiotechnology*. 14(9), 756–760. https://doi.org/10.1049/iet-nbt.2020.0084.

Keshu, R.M., Yadav, J., Balhra, M., Choudhary, S., Shanker, U., 2021. An updated review on synthetic approaches of green nanomaterials and their application for removal of water pollutants: Current challenges, assessment and future perspectives. *Journal of Environmental Chemical Engineering*. 9(6), 106763. https://doi.org/10.1016/j.jece.2021.106763

Khoramipour, K., Chamari, K., Hekmatikar, A.A., Ziyaiyan, A., Taherkhani, S., Elguindy, N.M., *et al.* 2021. Adiponectin: Structure, Physiological Functions, Role in Diseases, and Effects of Nutrition. Nutrients, 13, 1180. https://doi.org/10.3390/nu13041180

Kiritsakis, K., Kontominas, M.G., Kontogiorgis, C., Hadjipavlou-Litina, D., Moustakas, A., Kiritsakis, A., 2010. Composition and Antioxidant Activity of Olive Leaf Extracts from Greek Olive Cultivars. *Journal of the American Oil Chemists' Society*. 87(4), 369–376. https://doi.org/10.1007/s11746-009-1517-x

Koracevic, D., 2001. Method for the measurement of antioxidant activity in human fluids. *Journal of Clinical Pathology*. 54(5), 356–361. https://doi.10.1136/jcp.54.5.356.

Mahdy, E-SME-S., El-Mezayen, H.A., El-Mowafi, E-MA., 2017. Anti-Diabetic Effect of Balanites Aegyptiacea Leaves Extract (Heglig) by Regulation of Erythrocyte Glucose Uptake in Diabetic Patients Type 2 in Vitro. *The Egyptian Journal of Hospital Medicine*. 67(2), 528–535. https://doi.org/10.12816/0037802

Maritim, A. C., Sanders, R. A., & Watkins, J. B. (2003). Diabetes, oxidative stress, and antioxidants: A review. *Journal of Biochemical and Molecular Toxicology*. 17(1), 24–38. https://doi.org/10.1002/jbt.10058

Meighan, S., Gallop, R.J., Putman, M.S., Kelly, A., Marks, B.E., 2025. Alternative approaches to glucose measurements during oral glucose tolerance testing in youth with cystic fibrosis: a mixed methods pilot study. *Journal of Clinical & Translational Endocrinology*. 42(17), 100421. https://doi.org/10.1016/j.jcte.2025.100421

Menaka, K., Ramesh, A., Thomas, B., Kumari, S., 2009. Estimation of nitric oxide as an inflammatory marker in periodontitis. *Journal of Indian Society of Periodontology*. 13(2), 75-8. https://doi.org/10.4103/0972-124X.55842.

Mohammadi, A., Hashemi, N., Ghassabzadeh, M., Sharafi, A., Yazdinezhad, A., Danafar, H., 2025. Green synthesis and toxicological evaluation of zinc oxide nanoparticles utilizing Punica granatum fruit Peel extract: an eco-friendly approach. *Scientific Reports.* 15(1), 20853. https://doi.org/10.1038/s41598-025-05544-6.

Narayanan, K.B., Kim, H.D., Han, S.S., 2020. Biocompatibility and hemocompatibility of hydrothermally derived reduced graphene oxide using soluble starch as a reducing agent. *Colloids and Surfaces B: Biointerfaces*. 185, 110579. https://doi.org/10.1016/j.colsurfb.2019.110579.

Naser, D.K., Abbas, A.K., Aadim, K.A., 2020. Zeta Potential of Ag, Cu, ZnO, CdO and Sn Nanoparticles Prepared by Pulse Laser Ablation in Liquid Environment. *Iraqi Journal of Science*. 61(10), 2570–2581. https://doi.org/10.24996/ijs.2020.61.10.13

Nozhenko, Y., Asnani-Kishnani, M., Rodríguez, A.M., Palou, A., 2015. Milk Leptin Surge and Biological Rhythms of Leptin and Other Regulatory Proteins in Breastmilk. *PLoS One*. 10(12), e0145376. https://doi.org/10.1371/journal.pone.0145376

Osama, L., Yassa, N., Ghareeb, D., Elguindy, N.M., 2024. Antidiabetic, antioxidant, and anti-inflammatory effects of caffeic acid and zinc oxide nanoparticles against high-fat diet-treated rats. *Journal of the Medical Research Institute*. 45(3), 25–34. https://doi.org/10.21608/jmalexu.2024.317140.1028.

Pachaiappan, R., Rajendran, S., Ramalingam, G., Vo, D-V.N., Priya, P.M., Soto-Moscoso, M., 2021. Green Synthesis of Zinc Oxide Nanoparticles by *Justicia adhatoda* Leaves and Their Antimicrobial Activity. *Chemical Engineering & Technology*. 44(3), 551–558. https://doi.org/10.1002/ceat.202000470

Paoletti, F., Aldinucci, D., Mocali, A., Caparrini, A., 1986. A sensitive spectrophotometric method for the determination of superoxide dismutase activity in tissue extracts. *Analytical Biochemistry.* 154(2), 536–541. https://doi.org/10.1016/0003-2697(86)90026-6

Peng, Y-J., Shen, T-L., Chen, Y-S., Mersmann, H.J., Liu, B-H., Ding, S-T., 2018. Adiponectin and adiponectin receptor 1 overexpression enhance inflammatory bowel disease. *Journal of Biomedical Science*. 25(1), 24. https://doi.org/10.1186/s12929-018-0419-3.

Picó, C., Palou, M., Pomar, C.A., Rodríguez, A.M., Palou, A., 2022. Leptin as a key regulator of the adipose organ. *Reviews in Endocrine and Metabolic Disorders.* 23(1), 13–30. https://doi.org/10.1007/s11154-021-09687-5

Qadir, N.M., Ali, K.A., Qader, S.W., 2016. Antidiabetic Effect of Oleuropein from Olea europaea Leaf against Alloxan Induced Type 1 Diabetic in Rats. *Brazilian Archives of Biology and Technology*. 59, 1–10. https://doi.org/10.1590/1678-4324-2016150116.

Rahman, I., Kode, A., Biswas, S.K., 2006. Assay for quantitative determination of glutathione and glutathione disulfide levels using enzymatic recycling method. *Nature Protocols*. 1(6), 3159–3165. https://doi.org/10.1038/nprot.2006.378.

Saad, E. A., Hassanien, M. M., El-Hagrasy, M. A., & Radwan, K. H., 2015. Antidiabetic, hypolipidemic and antioxidant activities and protective effects of Punica Granatum peels powder against pancreatic and hepatic tissues injuries in streptozotocin induced IDDM in rats. *Journal of Pharmacy & Pharmaceutical Sciences*. 7(7):397-402.

Saad, E.A., Habib, S.A., Refai, W.A., Elfayoumy, A.A., 2017. Malondialdehyde, Adiponectin, Nitric Oxide, C-Reactive Protein, Tumor Necrosis Factor-Alpha and Insulin Resistance Relationships and Inter- Relationships in Type 2 Diabetes Early Stage is Metformin Alone Adequate in This Stage. *International Journal of Pharmacy and Pharmaceutical Sciences*. 9 (10), 176-181. https://doi.org/10.22159/ijpps.2017v9i10.21149

Sánchez-Gutiérrez, M., Bascón-Villegas, I., Rodríguez, A., Pérez-Rodríguez, F., Fernández-Prior, Á., Rosal, A., Carrasco, E., 2021. Article valorisation of olea europaea l. Olive leaves through the evaluation of their extracts: Antioxidant and antimicrobial activity. *Foods*. 10(5), 966. https://doi.org/10.3390/foods10050966

Shahidi, F., Danielski, R., 2024. Review on the Role of Polyphenols in Preventing and Treating Type 2 Diabetes: Evidence from In Vitro and In Vivo Studies. *Nutrients*. 16(18), 3159. https://doi.org/10.3390/nu16183159.

Sinha, A.K., 1972. Colorimetric assay of catalase. *Analytical Biochemistry*. 47(2), 389–394. https://doi.org/10.1016/0003-2697(72)90132-7.

Szabó, E., Kulin, A., Korányi, L., Literáti-Nagy, B., Cserepes, J., Somogyi, A., Sarkadi, B., & Várady, G., 2021. Alterations in erythrocyte membrane transporter expression levels in type 2 diabetic patients. *Scientific Reports*. 11(1), 2765. https://doi.org/10.1038/s41598-021-82417-8

Trinder, P., 1969. Determination of Glucose in Blood Using Glucose Oxidase with an Alternative Oxygen Acceptor. *Annals of Clinical Biochemistry.* 6(1), 24–27. https://doi.org/10.1177/000456326900600108.

Uchiyama, M., Mihara, M., 1978. Determination of malonaldehyde precursor in tissues by thiobarbituric acid test. *Analytical Biochemistry*. 86(1), 271–278. https://doi.org/10.1016/0003-2697(78)90342-1

Umrani, R.D., Paknikar, K.M., 2014. Zinc Oxide Nanoparticles Show Antidiabetic Activity in Streptozotocin-Induced Type 1 and 2 Diabetic Rats. *Nanomedicine*. 9(1), 89–104. https://doi.org/10.2217/nnm.12.205

Virgen-Ortiz, A., Apolinar-Iribe, A., Díaz-Reval, I., Parra-Delgado, H., Limón-Miranda, S., Sánchez-Pastor, E. A., Castro-Sánchez, L., Castillo, S. J., Dagnino-Acosta, A., Bonales-Alatorre, E., & Rodriguez-Hernández, A., 2020. Zinc oxide nanoparticles induce an adverse effect on blood glucose levels depending on the

dose and route of administration in healthy and diabetic rats. *Nanomaterials*. 10(10), 1–10. https://doi.org/10.3390/nano10102005

Yang, Q., Fu, C., Xiao, J., Ye, Z., 2017. Uric acid upregulates the adiponectin-adiponectin receptor 1 pathway in renal proximal tubule epithelial cells. *Molecular Medicine Reports*. 17(3), 3545-3554. https://doi.org/10.3892/mmr.2017.8315.